Published in final edited form as:
J Mater Chem. 2011 January 1; 2011(48): 19293–192301. doi:10.1039/C1JM13754A.

New ratiometric optical oxygen and pH dual sensors with three emission colors for measuring photosynthetic activity in Cyanobacteria

Hongguang Lu, **Yuguang Jin**, **Yanqing Tian***, **Weiwen Zhang***, **Mark R. Holl**, and **Deirdre R. Meldrum**
Center for Biosignatures Discovery Automation, The Biodesign Institute, Arizona State University, PO Box 875801, Tempe, AZ 85287-5801

Abstract

Photosynthetic algae and cyanobacteria have been proposed for producing biofuels through a direct photoconversion process. To accelerate the efforts of discovering and screening microbes for biofuel production, sensitive and high throughput methods to measure photosynthetic activity need to be developed. Here we report the development of new ratiometric optical oxygen and pH dual sensors with three emission colors for measuring photosynthetic activities directly. The dual sensor system can measure oxygen (O_2) generation and pH increase resulted from carbon dioxide (CO_2) consumption simultaneously. The sensor was prepared by a copolymerization of three monomeric probes, an intra-reference probe (**IRP**) which does not respond to pH or O_2, a probe for pH sensing (**pHS**), and an O_2 probe for O_2 sensing (**OS**) with 2-hydroxyethyl methacrylate (HEMA) and acrylamide (AM). After polymerization, the three probes were chemically immobilized in an ion and O_2 permeable poly(2-hydroxyethyl methacrylate)-*co*-polyacrylamide (PHEMA-*co*-PAM) matrix. The resulted sensing films (membranes) exhibited three emission colors with well separated emission spectra, covering blue, green, and red emission windows, under 380 nm light excitation. Responses of the sensors to pH and dissolved O_2 were investigated in buffers and cyanobacterial cell cultures (*Synechocystis* sp. PCC 6803). In spite of the strong autofluorescence from cyanobacteria, the sensors were able to determine the pH values and dissolved O_2 concentrations accurately and reproducibly. The measured results using the optical sensors were well in accordance with measurements using electrodes with minimal experimental variations. The sensors were further applied for evaluation of photosynthetic activities of *Synechocystis* sp. PCC 6803 at the exponential and stationary phases. The results were consistent with biological observation that the photosynthetic activity in the exponential phase was higher than that in the stationary phase.

1. Introduction

High oil prices and growing concerns over national security and climate change are driving investment and innovation in the renewable biofuels sector.[1–3] Photosynthetic algae and cyanobacteria have been proposed for producing biofuels through a direct photoconversion process.[4] The efficiency of the biofuel production depends on the photosynthetic activity of microbes, *e.g.*, the ability of consumption of CO_2 and the generation of oxygen (O_2).5 Several methods have been developed and applied in the past to measure photosynthetic activities.[6] Typically these methods involve measurement of single parameter, either O_2

*To whom correspondence should be addressed: Dr. Yanqing Tian (Yanqing.Tian@asu.edu) or Dr. Weiwen Zhang (Weiwen.Zhang@asu.edu), Center for Biosignatures Discovery Automation, The Biodesign Institute, Arizona State University, PO Box 875801, Tempe, AZ 85287-5801.

generation or CO_2 consumption. These methods include: *a*) the dry matter accumulation; *b*) manometric measurement of the pressure of CO_2 or O_2 in an isolated chamber containing photosynthetic organisms; *c*) use of electrodes to measure dissolved oxygen and CO_2, or change in pH; *d*) CO_2 and/or O_2 gas exchange; *e*) CO_2 isotope measurement; and *f*) measurement of autofluorescence from chlorophyll and/or chloroplast.[6] Among them, measurements of the CO_2 consumption and/or O_2 generation using electrodes[7] are currently the most popular technique. Although these methods have been applied successfully in the past, they are typically time- and labor-intensive, often require special devices, and their measurement throughput is typically low. Also the above mentioned methods are difficult to measure two parameters simultaneously. For example, two separate electrodes have to be applied in parallel to simultaneously measure pH and oxygen concentration.

On the other hand, simultaneous detection of pH and dissolved oxygen (DO) concentrations is important for monitoring drinking water quality, determining freshness of food, and understanding cell metabolism, cell respiration rate, cell health and diseases including cancer. Fluorescence-based optical sensors, where organic and polymeric fluorophores are deposited onto different surfaces, can be miniaturized easily to sub-micrometer scale, and have been applied to measure pH and O_2 changes in both small and large dimension scales.[8, 9, 10] The methods have been demonstrated to be sensitive, highly reproducible, readily to be developed into high throughput formats, and feasible to measure two or more parameters simultaneously. Especially, when using optical sensors for noninvasive *in vitro* or *in vivo* biological studies, the optical sensors showed significant advantages over the electrodes and colorimetric approaches.[9, 11] Although many individual oxygen [8, 9, 12 – 18] and pH [19, 20, 21, 22] sensors have been developed, few fluorescence-based optical dual pH and oxygen sensors were reported.[9, 11, 23 – 26] Initially, these dual sensors were usually based on fluorescein-derivatives as pH sensors and platinum porphyrins as oxygen sensors which were physically dispersed in suitable polymer matrices.[9, 11, 23–25] Leaching of the probes from the matrix is a significant issue. To alleviate this problem, a dual sensor with a chemical conjugation of the probes into the matrix was developed.[26] These sensors were studied as new materials and/or applied for evaluation of pH change and/or oxygen consumptions during eukaryotic and prokaryotic cell cultures. However, there is no report about the development of new dual pH and oxygen sensors for photosynthetic activity evaluation. In this work, we made initial efforts to synthesize new dual optical pH and O_2 sensors suitable for evaluating the photosynthetic activities through the measurements of the pH and DO concentration changes simultaneously in cell culture media.

Green algae and cyanobacteria contain significant amounts of chlorophyll, nicotinamide adenine dinucleotide phosphate (NADPH), and other pigments for photosynthesis, which exhibit strong autofluorescence under light excitation.[27–29] Therefore, the optical sensors developed for pH and DO measurements in photosynthetic organism need to possess stronger fluorescence intensities in order to alleviate the background interference by the chlorophyll and other pigments. To achieve this goal, new dual pH and O_2 sensors in the thin film states were developed and they showed much higher fluorescence intensities than the autofluorescence background of cyanobacteria under the same optical conditions. Further, to minimize the background influence and getting accurate measurement results, the new dual pH and O_2 sensor system exhibits three emission colors by integrating a blue emitter, called intra reference-probe (**IRP**), which does not respond to either pH or O_2, with a green emitter for pH sensing (**pHS**) and a red emitter for O_2 sensing (**OS**). Thus the blue emission can be used as an intra-reference for pH and O_2 sensing using the ratiometric method.[30–33] Ratiometric method is based on the measurement of two probes simultaneously, one that is sensitive to the analyte of interest, and a second that is not, and to then take the ratio of the two.[30–33] The ratiometric method has been known to increase the measurement accuracy and to alleviate the environmental influences, such as fluctuations in

excitation source intensity, variance in probe concentration, and uncontrollable variations in background fluorescence.

Herein, we design a new sensor system with three emission colors. Intensity-based ratiometric measurement was applicable for the pH and dissolved O_2 measurements. Detailed chemical structures of the **IRP** with blue emission, pH probe for pH sensing (**pHS**) with green emission, and O_2 probe for O_2 sensing (**OS**) with red emission are given in Figure 1. Each of the three compounds possesses at least one methacrylate moiety, enabling the monomeric probe to be polymerized with 2-hydroxylethyl methacrylate (HEMA) and acrylamide (AM) to form ion and oxygen permeable sensing films. Poly(2-hydroxylethyl methacrylate)-*co*-polyacrylamide (PHEMA-*co*-PAM) polymers have been widely used as contact lens[34, 35] due to their good ion and oxygen permeability. We have used PHEMA-*co*-PAM matrices for pH and oxygen sensing studies.[22, 26, 36] We report here the preparation of the tri-color dual pH and O_2 sensing films, characterization of the sensing responses, and the application of the sensing films to evaluate the pH and O_2 changes of the *Synechocystis* sp. PCC 6803 from different growth stages at room temperature.

2. Experimental

2.1. Materials

pHS and **OS** (Figure 1) were synthesized according to our previous procedures.[22, 26, 36] Detailed synthesis of **IRP** was described in the supporting material S-Scheme 1. 2-Hydroxylethyl methacrylate (HEMA), acrylamide (AM), polyethylene glycol dimethacrylate (PEG dimethacrylate, M_n = 550), 2-(methacryloyloxy)ethylsulfonic acid sodium salt (MESA), trimethylsilylpropyl acrylate (TMSPA), azobisisobutyronitrile (AIBN), and *N, N′*-dimethyl formamide (DMF) are commercially available from Sigma-Aldrich (St. Louis, MO) and were used without further purification. Britton-Robinson (B-R) buffers with different pH values were composed of acetic acid, boric acid, phosphoric acid, and sodium hydroxide. A mixture of oxygen and nitrogen gas (AIR Liquide America LP, Houston, TX) was used to saturate the B-R buffers and the cell culture media to control precisely the dissolved oxygen concentrations through a custom-built, in-line, digital gas flow controller.

2.2. Instruments

A Varian liquid-state NMR operated at 400 MHz for ^{1}H NMR was used for NMR spectra measurements. High resolution mass spectrometry (HRMS) was performed by the Mass Spectrometry Laboratory in Arizona State University (ASU). An oxygen plasma cleaner (Harrick Plasma, Ithaca, NY) was used for quartz glass surface activation. A Shimadzu UV-3600 UV-Vis-NIR spectrophotometer (Shimadzu Scientific Instruments, Columbia, MD) was used for absorbance measurements. A Shimadzu RF-5301 spectrofluorophotometer was used for fluorescence measurements. For convenient measurements of the films in liquid solutions, quartz glass was cut with a dicing saw into squares of 1.31cm × 1.31cm, which can fit diagonally into a quartz fluorescence cuvette to enable the sensing film be positioned at an angle of 45° to the excitation light. Life science UV/Vis spectrophotometer, Beckman Du@530, was used for the bacterial optical density (OD) measurement. A digital pH meter (Thermo Electron Corporation, Beverly, MA) calibrated at room temperature (23 ± 2°C) with standard buffers of pH 10.01, 7.00, and 4.01 was used to determine pH values. A dip-type O_2 microelectrode (Model MI-730, Microelectrodes, Inc., Bedford, New Hampshire) was used to determine dissolved O_2 concentrations.

2.3. Sensor film preparation

The thin films were prepared according to our published protocol.[22, 26, 36] A schematic drawing is given in Supporting S-Figure 1. Briefly, 1.4 mg of the **IRP**, 800 mg of HEMA, 150 mg of AM, 50 mg of PEG dimethacrylate, 150 mg of MESA, and 10 mg of AIBN were dissolved in 1 mL DMF as the stock solution of the intra-reference probe. 1.6 mg of the **OS**, 800 mg of HEMA, 150 mg of AM, 50 mg of PEG dimethacrylate, 150 mg of MESA, and 10 mg of AIBN were dissolved in 1 mL DMF as the stock solution of the oxygen probe. 2.0 mg of the **pHS**, 800 mg of HEMA, 150 mg of AM, 50 mg of PEG dimethacrylate, 150 mg of MESA, and 10 mg of AIBN were dissolved in 1 mL DMF and 100 μL water as the stock solution of pH probe. The addition of 100 μL water is to enable a complete dissolving of the MESA in the solution. In order to get reasonable peak intensity ratios among the three probes, the three probes' stock solutions were mixed according a ratio of 8 μL : 10 μL : 200 μL of the **IRP**, **pHS**, and **OS** stock solutions. 10 μL of the **IRP**/**pHS**/**OS** stock solutions were added onto the surface of the TMSPA-modified quartz glass and covered with a clean but untreated cover slip to make a sandwich structure. Using TMSPA to modify the quartz glass was to enable the sensors and matrices to be chemically grafted onto a quartz substrate. To produce the polymer thin film with good mechanical stability, PEG dimethacrylate was used as a crosslinker. To further increase the water and ion permeability, AM was added as a second monomer for the thin film formation. The thickness was controlled using 25 μm Kapton tape (DuPont, Wilmington, DE). The sandwich set-up was placed into a vacuum oven, which was then evacuated and refilled with nitrogen three times. Polymerization was carried out under nitrogen at 80°C for 1.5 hours in the oven. The quartz glasses with polymer membranes were removed from the oven, with Kapton tape and non-surface modified glass being removed from the polymerized membrane surface. The polymer membranes on the quartz glasses were washed three times using methanol to remove any remaining non-polymerized monomers and residual DMF. The films were dried and stored in the dark at room temperature.

2.4. Cultivation of photosynthetic microbes

Synechocystis sp. PCC 6803 was obtained from American Type Culture Center (ATCC) and was grown phototrophically in liquid BG11 medium at 30°C under 300 $\mu E/m^2s$ of white light.[37]

2.5. Sensors toxicity and attachment

To determine any possible cellular toxicity of the sensors, we cultivated *Synechocystis* sp. PCC 6803 in 250 mL flasks with or without the sensor thin films (controls) for up to 3 days. The cell optical densities were comparatively determined at 730 nm (OD_{730}). In addition, throughout the growth time courses, cells were also taken for microscopic examination. Moreover, the sensor thin films were also taken out, rinsed gently with BG11 medium and then were monitored for possible cell attachment.

2.6. In-site measurement of the pH and O_2 concentration in *Synechocystis* sp. PCC 6803

Cells in the middle exponential growth and late stationary growth phases were harvested by centrifugation (Beckman Coulter 64R centrifuge) at 4000 rpm for 10 min at room temperature. The cell pellets were washed twice gently with sterilized fresh BG11 medium, and then re-suspended in sterilized fresh BG11 medium. The cell optical density in suspension was first determined at 730 nm (OD_{730}) and then adjusted to make sure each measurement used the equal number of cells. Three cell optical densities at 730 nm used in activity analyses were 1.50 (approx. 1.5×10^8 cell/mL), 0.75 (approx. 7.5×10^7 cell/mL), and 0.50 (approx. 5×10^7 cell/mL). Sensing films were immersed inside 3.8 mL of the cell suspension in a 4 mL transparent plastic cuvette. The cells in the cuvettes were exposed to

white light (300 μE/m^{2}s) for a period of time (0 – 90 min testing time). The fluorescence intensity from the sensor film in the cuvette was measured using spectrofluorophotometer using 380 nm as the excitation wavelength. Emission was collected from 400 to 700 nm.

3. Results and discussion

3.1. Design of sensors

The sensor film contains three probes with three different emission colors. The blue emission is for **IRP**, which does not respond to either pH or O_2. **IRP** was constructed from a fluorene trimer (Figure 1). Fluorene oliogomers and polymers are well known to show blue emission and the materials are widely applied in the organic light emitting diode field.[38] **pHS** is a derivative of amino-naphthalimide showing the emission in the green spectral window.[22,26] This sensor will follow a photo-induced electron transfer (PET) mechanism and show stronger fluorescence intensity at low pH value and weaker emission at high pH value. At higher pH value, PET occurs from the lone electron pair of the NCH_3 group to the acceptor amino-naphthalimide fluorophore, making the sensor weakly fluorescent. At lower pH, however, the protonation of the amino group diminishes the PET effect and, in turn, leads to restoration of the fluorescence originating from the fluorophore, 4-amino-1, 8-naphthalimide.[22,26] Hence, a remarkable increase in fluorescence intensity was observed with a decrease in pH. The O_2 probe (**OS**) is a platinum porphyrin derivative exhibiting red emission, which can be quenched by O_2 through triplet-triplet energy transfer.[26,36] The three optical probes have well separated spectral windows and can be excited using a same excitation wavelength, 380 nm (Figure 2).

3.2. pH and O_2 responses in B-R buffer

Figure 2A shows absorption spectra of the sensing film. A major peak around 390 nm and two small peaks at 510 and 530 nm were observed. The 390 nm peak is the overlay of the absorbencies of **IRP** (maximum at 355 nm), **pHS** (maximum at 390 nm) and the Soret-band of **OS** (maximum at 395 nm) (Supporting S-Figure 2). The two small peaks at 508 and 540 nm are the Q-bands of the O_2 probe.[36] The peaks at 508 and 540 nm have almost no change upon the pH value. This is because **OS** has no pH sensitive moiety. Slight absorbance changes at 390 nm were observed, which is probably due to the small absorbance changes of **pHS**[21] by pH because the absorbance of **IRP** and the Soret-band of **OS** do not change with pH value. Since all the three probes have overlapped absorbance in the range of 350 to 440 nm with a maximum around 390 nm, they can be excited at single wavelength in this range. In order to collect all the emissions of the three probes, 380 nm was chosen. Figure 2B shows the emission spectra of a sensor film at different pH values. The blue emission at 421 nm from **IRP** doesn't change with pH value. The emission at 521 nm decreased with the increase of pH value, showing a good pH response of the sensing film due to **pHS**. The red emission at 650 nm is from **OS**, which does not change with pH values.

Figure 2C shows the sigmoidal plots (Boltzmann fitting, equation 1) of the sensor film using two different calculation approaches.

$$\frac{I}{I_0}=\frac{m1-m2}{1+\exp(\frac{pH-pK_a'}{p})}+m2 \quad (1)$$

Approach 1 is the sigmoidal plot using the intensity change of the **pHS** at 521 nm. Where, I and I_0 are the fluorescence intensities measured at varying pH values and at the highest pH value (pH 10) used during the calibration, respectively. $m1$, $m2$, pK_a', and p are empirical parameters describing the initial value ($m1$), the final value ($m2$), the point of inflection

(pK_a'), and the width (p) of the sigmoidal curve. The apparent pK_a value (pK_a') was 8.53 the sensor film in B-R buffer. The fitting was highly reliable with a correlation coefficient (R^2) of 0.994.

Approach 2 is the plot using the ratiometric intensity ratios by I_{521}/I_{421} against pH values. I_{521} is the emission intensity at 521 nm from the pH sensor. I_{421} is the emission intensity at 421 nm from the **IRP**. The pK_a value was calculated to be 8.55. The quite close pK_a values calculated using these two approaches indicate the reliability of ratiometric approach.

Figure 2D shows the absorption change of a sensor film under different dissolved O_2 concentration. The absorption has no change upon the different O_2 conditions, indicating there was no chemical reaction between the O_2 molecules and the three probes. The emission intensities at 421 nm and 521 nm have no change under the various oxygen conditions (Figure 2D). A marked dependence of fluorescence intensities at 650 nm on O_2 concentrations was observed (Figure 2E), showing the emission of the O_2 sensor was physically quenched by O_2. However, the **IRP** and **pHS** were not affected by O_2 concentration changes.

The intensity ratio (I_0/I) curve (Figure 2F) follows the Stern-Volmer equation:

$$\frac{I_0}{I}=1+K_{SV}[O_2] \quad (2)$$

where K_{SV} is Stern-Volmer quenching constant and [O_2] is the dissolved O_2 concentration. I_0 and I are the steady-state fluorescence signals measured in the presence of nitrogen and various oxygen concentrations generated by controlled gas bubbling, respectively. The dissolved O_2 concentration [O_2] is proportional to the partial pressure of O_2, pO_2, in the gas used to saturate the liquid. At 23°C under air condition with the O_2 partial pressure of 21.3 kPa, the [O_2] in the B-R buffer is 8.6 mg L^{-1}.

Ratiometric approach using the intensity ratios at 650 nm and 421 nm (I_{421}/I_{650}) also follows linear Stern-Volmer equation (Figure 2F). The linear Stern-Volmer O_2 response suggests the uniform O_2 probe's distribution in the sensing membrane, which is in accordance with our previous studies using the PHEMA-*co*-PAM matrices.[26, 36]

3.3. Effect of cyanobacterial autofluorescence on pH and O_2 measurements

Photosynthetic microbes are well known to contain various pigments, most of them are directly required for photosynthetic activity and can generate autofluorescence.[27, 28, 39] In several early studies, autofluorescence has been suggested as one of the major hurdles in developing fluorescent sensor based assay for photosynthetic microbes.[40] To determine the effect of cyanobacterial autofluorescence on our fluorescent-dyes based assays, we performed the assays with *Synechocystis* sp. PCC 6803 of different cell densities in the measurement system. In the experiments, pH value of the bacteria-containing BG11 medium was manipulated using hydrochloric acid and sodium hydroxide aqueous solution. O_2 concentration was adjusted by saturating the cyanobacteria-containing BG11 media with mixtures of oxygen and nitrogen gases. Through tuning of the pH values and dissolved O_2 concentrations in the systems, the sensitivity and reproducibility of the sensors were examined.

Under the excitation at 380 nm, the *Synechocystis* sp. PCC 6803 exhibits autofluorescence at two maxima around 460 nm and 660 nm due to NADPH[27,28] and chlorophyll,[6] respectively. Figure 3 showed the autofluorescence and the sensor responses in the cell density with an OD_{730} of 0.5, corresponding to the cell density of 5×10^7 cells/mL. Other

titrations using cell densities with an OD_{730} of 0.75 and 1.5 were given in the supporting materials (S-Figures 3 and 4).

The autofluorescence maximum at 660 nm is overlapped completely with that of the O_2 sensor. Although it was a critical concern initially, we later demonstrated that at the cell densities we tested, the autofluorescence intensity ($I_{\text{auto }650}$) is less than 5% of the fluorescence intensity from the sensing film ($I_{\text{O2-sensor }650}$) at the oxygenated condition. Thus, the effect of autofluorescence peak at 660 nm on the measurement accuracy of our dual sensor system is very minimal.

The autofluorescence at 460 nm is in between the emissions maxima of **IRP** and **pHS.** This autofluorescence varies with pH and O_2 concentration changes (Figure 3A and 3D) as well as increases with cell density increases. In addition, this autofluorescence is broad and has overlay with the emissions of **IRP** and **pHS**. Because of all these factors, the autofluorescence at 460 nm affected sensors pH sensitivity significantly. pH sensitivities decreased with the increase of cell densities (Figure 2C via Figure 3C, S-Figure 3C, and S-Figure 4C). This autofluorescence also affected oxygen sensing at high cell density of OD_{730} at 1.5. At this high cell concentration, the responses of **OS** to O_2 did not follow well the linear Stern-Volmer equation (S-Figure 4F). Results showed that cell density with OD_{730} of 0.5 is the optimized condition to minimize the influence of cyanobacterial autofluorescence, and at the same time to obtain sensitive and reproducible measurements. Therefore, all the following experiments for photo-activities evaluations were carried out using bacteria with OD_{730} of 0.5.

It should be noted here that, when *Synechocystis* sp. PCC 6803 was included in the measurement systems, during the pH titration process, the oxygen concentration increase slightly, as shown by the decrease of the intensity at 660 nm (Figure 2B, S-Figure 3B, and S-Figure 4B). During the oxygen titration process, increase of pH values was observed, as shown by the decrease of the emission intensity at 521 nm (Figure 2E, S-Figure 3E, and S-Figure 4E). Because the pH sensor does not respond to O_2 or the O_2 sensor does not respond to pH either in buffers, the complex behaviors of the sensors in cyanobateria cultures indicated the simultaneous O_2 generation and CO_2 consumption of the cyanobacteria in the titration process.

To test reproducibility and the titration accuracy, four individual films were investigated and the results showed that all the four films had similar pK_a and sensitivities, demonstrating they are highly reliable (S-Figure 5). In addition, the toxicity assay also showed that for the testing period of 2 days, sensors have not caused any negative effect on *Synechocystis sp. PCC* 6803 cells based on both cell growth measurements (Supporting materials, S-Figure 6). Moreover, no cell attachment was found on the thin films after *Synechocystis sp. PCC* 6803 cultivated with thin films for 10 days (data not shown).

3.4. Application of dual sensors for the measurements of the photosynthetic activity in *Synechocystis* sp. PCC 6803

To validate the application of the sensor system for photosynthetic microbes, we performed experiments using *Synechocystis* sp. PCC 6803 from different growth conditions. Results in Figure 4 showed the measurements of pH and O_2 for *Synechocystis* sp. PCC 6803 of exponential phase (A, B, and C) and stationary phase (D, E, and F). The measurements were performed under light irradiation (white light at 300 $\mu E/m^2s$) at room temperature. Each sensor film was immersed in 3.8 mL cell suspension with cell density at OD_{730} of 0.5 in a 4 mL cuvette. Three sensors and measurements were performed in parallel. For efficient monition of the pH change and O_2 generation, the cuvettes were sealed with a transparent cap to prevent CO_2 and O_2 exchanges with air. At the end of the measurements, the cuvettes

were opened and the end-point pH and dissolved O_2 concentrations were measured immediately using pH and O_2 electrodes. Table 1 showed the comparison of the data obtained from the optical sensors and electrodes, and in general very good consistence was observed between the two measurement methods with difference for pH measurements of ± 0.29, and oxygen concentration of ± 1.2 mg/L.

Figure 4G and 4F gave the comparison of time dependent pH increase and O_2 generation using the average pH values and O_2 concentrations measured by the films of F1, F2 and F3 for exponential phase and films of F4, F5, and F6 for stationary phase, respectively. It was found rates of pH value increases and oxygen generations of *Synechocystis* sp. PCC 6803 in stationary phases were slower than those in exponential phase (Figure 4G) after 20 minutes exposure to light, consistent with the relatively low photosynthetic activity of cyanobacterial cells from stationary phase. The results demonstrated that the sensors can be used for accurate measurements of the pH values and dissolved oxygen of the system directly for photosynthetic microbes.

3.5. Discussion for the future materials development

The short excitation wavelength (380 nm) is a weakness of the current sensor, since the short excitation wavelength will generate strong autofluorescence. The current sensing materials were interfered by high concentrated bacteria with an OD of higher than 0.75. Further improvement of the sensing performance using other pH sensors and intra-reference probes which can be excited by excitation wavelength such as 488 nm or even longer is necessary. The next generation of the sensor should be applicable for *in-situ* high concentration cyanobacterial photosynthetic activity measurement. Long term stability of the sensor system needs to be considered. The current sensor thin film is very stable in the B-R buffer at pH of 7.2 for longer than two months, however, only stable for 2 days at the cell culture condition because of the strong basic condition (pH > 10). With a longer incubation time than 2 days with cyanobacteria, the sensor came off from the substrate. Further improvement of the sensors' long term stability at the basic condition using amide bonds to replace the ester bonds will be carried out.

4. Conclusions

Herein we reported the preparation and characterization of novel dual pH and O_2 sensing films with three emission colors, blue, green and red, and their applications in directly measuring photosynthetic activities in cyanobacterial cells. The blue emission was not responsive to pH or O_2, which serves as an intra-reference probe. No cross-response was observed between pH ad O_2 sensors. The sensing responses were affected significantly by cell densities used due to the autofluorescence of cyanobacterial cells, and it was found the optimal cell density for sensitive and reproducible measurements was OD_{730} of 0.5. We validated the sensing systems using *Synechocystis* sp. PCC 6803 from both exponential and stationary phases. In addition, we also compared the data measured from optical sensors and electrodes. Results showed that the two measurements generated very similar results with small differences – (± 0.29 for pH values, ± 1.2 mg/L for oxygen concentrations). These results demonstrated that even for photosynthetic microbes with strong autofluorescence, by optimizing the cell density and measurement conditions, accurate pH values and dissolved oxygen concentrations can be determined using the sensing film we developed. Given the facts that the methods are inexpensive and easily established, we anticipate the methods can be a very good tool for the research fields of photosynthetic microbes. The method can also be amenable to a high throughput format, which will eventually enhance our understanding of physiology and biochemistry of photosynthetic microbes and relevant biofuels research in many ways.

Supplementary Material

Refer to Web version on PubMed Central for supplementary material.

Acknowledgments

Financial support was provided by the Microscale Life Sciences Center, a NIH Center of Excellence in Genomic Sciences at Arizona State University (Grant 5P50 HG002360, Dr. Deirdre Meldrum, PI, Director). Hongguang Lu was funded by a China Scholarship Council scholarship program for oversea graduate students.

References

1. Wirth TE, Gray CB, Podesta JD. Foreign Affairs. 2003; 82:132–155.
2. Kerr RA, Service RF. Science. 2005; 309:101. [PubMed: 15994547]
3. Hill J, Nelson E, Tilman D, Polasky S, Tiffany D. Proc Natl Acad Sci USA. 2006; 103:11206–11210. [PubMed: 16837571]
4. Atsumi S, Higashide W, Liao JC. Nat Biotechnol. 2009; 27:1177–1180. [PubMed: 19915552]
5. Angermayr SA, Hellingwerf KJ, Lindblad P, de Mattos MJT. Curr Opin Biotechnol. 2009; 20:257–263. [PubMed: 19540103]
6. Millan-Almaraz JR, Guevara-Gonzalez RG, Romero-Troncoso RJ, Osornio-Rios RA, Torres-Pacheco I. Afr J Biotechnol. 2009; 25:7340–7349.
7. Clark LC. Trans Am Soc Artif Intern Organs. 1956; 2:41–48.
8. Amao Y. Microchim Acta. 2003; 143:1–12.
9. Nagl S, Wolfbeis OS. Analyst. 2007; 132:507–511. [PubMed: 17525805]
10. Vilozny B, Schiller A, Wessling RA, Singaram B. J Mater Chem. 2011; 21:7589–7595.
11. Wolfbeis OS. J Mater Chem. 2005; 15:2657–2669.
12. Mitsubayashi K, Wakabayashi Y, Murotomi D, Yamada T, Kawase T, Iwagaki S, Karube I. Sens Actuators B. 2003; 95:373–377.
13. Wang XD, Chen X, Xie ZX, Wang XR. Angew Chem Int Ed. 2008; 47:7450–7453.
14. Payne SJ, Fiore GL, Fraser CL, Demas JN. Anal Chem. 2010; 82:917–921. [PubMed: 20050641]
15. McDonagh C, MacCraith BD, McEvoy AK. Anal Chem. 1998; 70:45–50. [PubMed: 21644598]
16. Borisov SM, Vasylevska AS, Krause C, Wolfbeis OS. Adv Funct Mater. 2006; 16:1536–1542.
17. Köse ME, Carrol BF, Schanze KS. Langmuir. 2005; 21:9121–9129. [PubMed: 16171341]
18. Tian Y, Shumway BR, Gao W, Youngbull C, Holl MR, Johnson RH, Meldrum DR. Sens Actuators B. 2010; 150:579–587. and references therein.
19. Fry DR, Bobbitt DR. Microchem J. 2001; 69:123–131.
20. Lobnik A, Oehme I, Murkovic I, Wolfbeis OS. Anal Chim Acta. 1998; 367:159–165.
21. Niu CG, Zeng GM, Chen LX, Shen GL, Yu RQ. Analyst. 2004; 129:20–24. [PubMed: 14737578]
22. Tian Y, Su F, Weber W, Nandakumar V, Shumway BR, Jin Y, Zhou X, Holl M, Johnson RH, Meldrum DR. Biomaterials. 2010; 31:7411–7422. and references therein. [PubMed: 20619451]
23. Vasylevska GS, Borisov SM, Krause C, Wolfbeis OS. Chem Mater. 2006; 18:4609–4616.
24. Schröder CR, Polerecky L, Klimant I. Anal Chem. 2007; 79:60–70. [PubMed: 17194122]
25. Kocincova AS, Arain SN, Krause C, Borisov SM, Arnold M, Wolfbeis OS. Biotechnol Bioeng. 2008; 100:430–438. [PubMed: 18383124]
26. Tian Y, Shumway BR, Youngbull AC, Li Y, Jen AK-Y, Johnson RH, Meldrum DR. Sens Actuators B. 2010; 147:714–722.
27. Mi H, Klughammer C, Schreiber U. Plant Cell Physiol. 2000; 41:1129–1135. [PubMed: 11148271]
28. Steigenberger S, Terjung F, Grossart HP, Reuter R. EARSel eProceedings. 2004; 3:18–25.
29. Kühl M. Methods Enzymol. 2005; 397:166–199. [PubMed: 16260291]
30. Xu H, Aylott JW, Kopelman R, Miller TJ, Philbert MA. Anal Chem. 2001; 73:4124–4133. [PubMed: 11569801]

31. Kermis HR, Kostov Y, Harms P, Rao G. Biotechnol Prog. 2002; 18:1047–1053. [PubMed: 12363356]
32. Schaeferling M, Duerkop A. Springer Series on Fluorescence. 2008; 5:373–414.
33. Lee S, Ibey BL, Cote GL, Pishko MV. Sens Actuators B. 2008; 128:388–398.
34. Fornasiero F, Krull F, Prausnitz JM, Radke CJ. Biomaterials. 2005; 26:5704–5716. [PubMed: 15878376]
35. Wang Y, Tan G, Zhang S, Guang Y. Appl Surf Sci. 2008; 255:604–606.
36. Tian Y, Shumway BR, Meldrum DR. Chem Mater. 2010; 22:2069–2078. [PubMed: 20352057]
37. Yamasato A, Satoh K. Plant Cell Physiol. 2001; 42:414–418. [PubMed: 11333312]
38. Zhong C, Duan C, Huang F, Wu H, Cao Y. Chem Mater. 2011; 23:326–340.
39. Wang C, Xing D, Chen Q. Biosens Bioelectron. 2004; 20:454–459. [PubMed: 15494225]
40. Yagi K. Appl Microbiol Biotechnol. 2007; 73:1251–1258. [PubMed: 17111136]

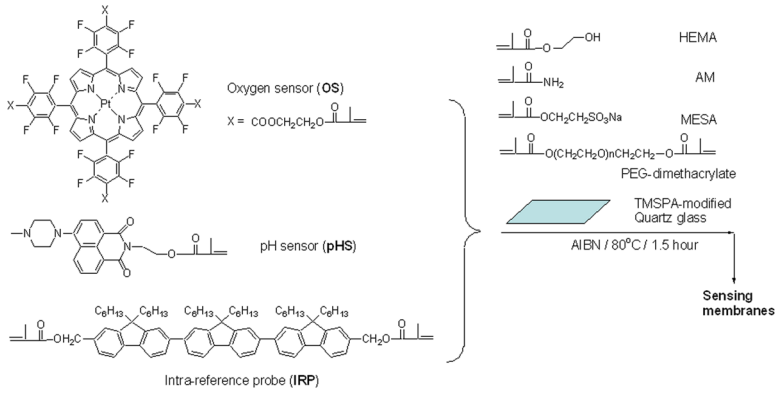

Figure 1.
Chemical structures of the three probes, and the outline of preparation of the sensing films.

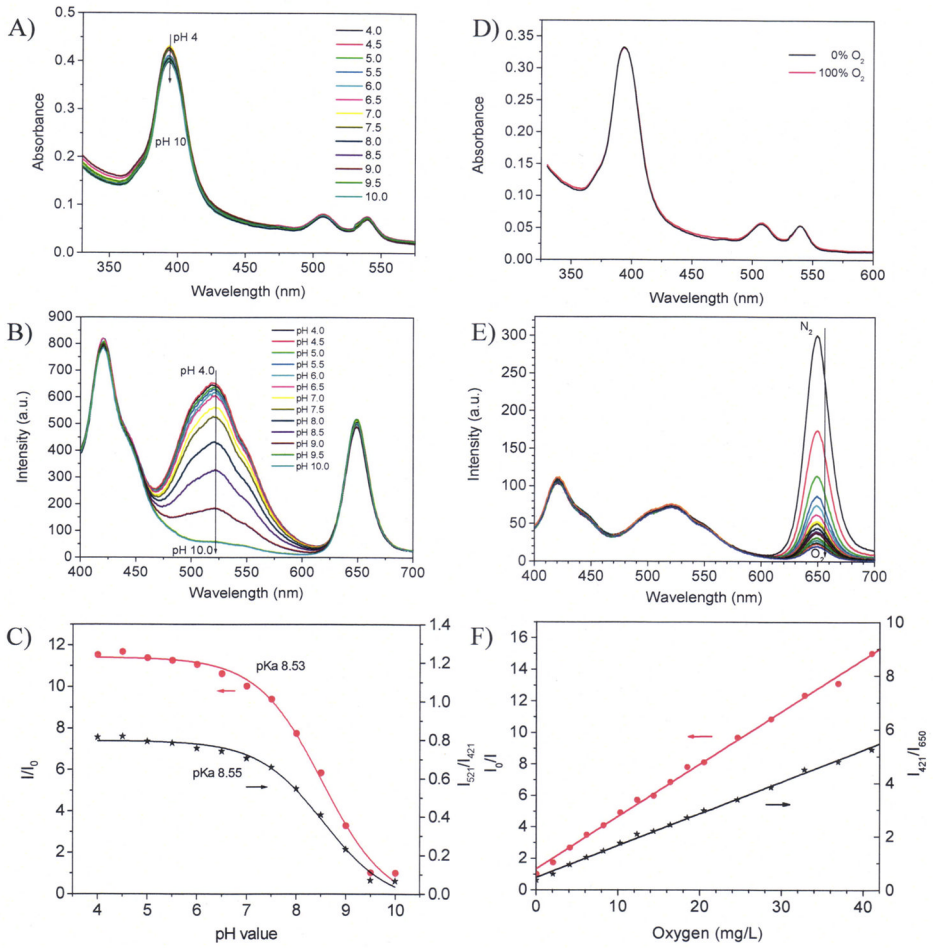

Figure 2.

Sensor responses in buffer. A) absorption spectra at different pH values; B) emission spectral changes at different pH values in air saturated buffers (under oxygen partial pressure of 21 kPa corresponding to [O_2] of 8.6 mg/L); C) Sigmoidal plots of the pH responses using the single pH sensor emission intensities at 521 nm and the ratiometric ratios at 521 nm and 421 nm; D) absorption spectra at deoxygenated and oxygenated conditions; E) emission spectral changes at different oxygen concentrations; F) Stern-Volmer plots of oxygen responses using the single oxygen sensor emission intensities at 650 nm and the ratiometric ratios at 650 nm and 421 nm.

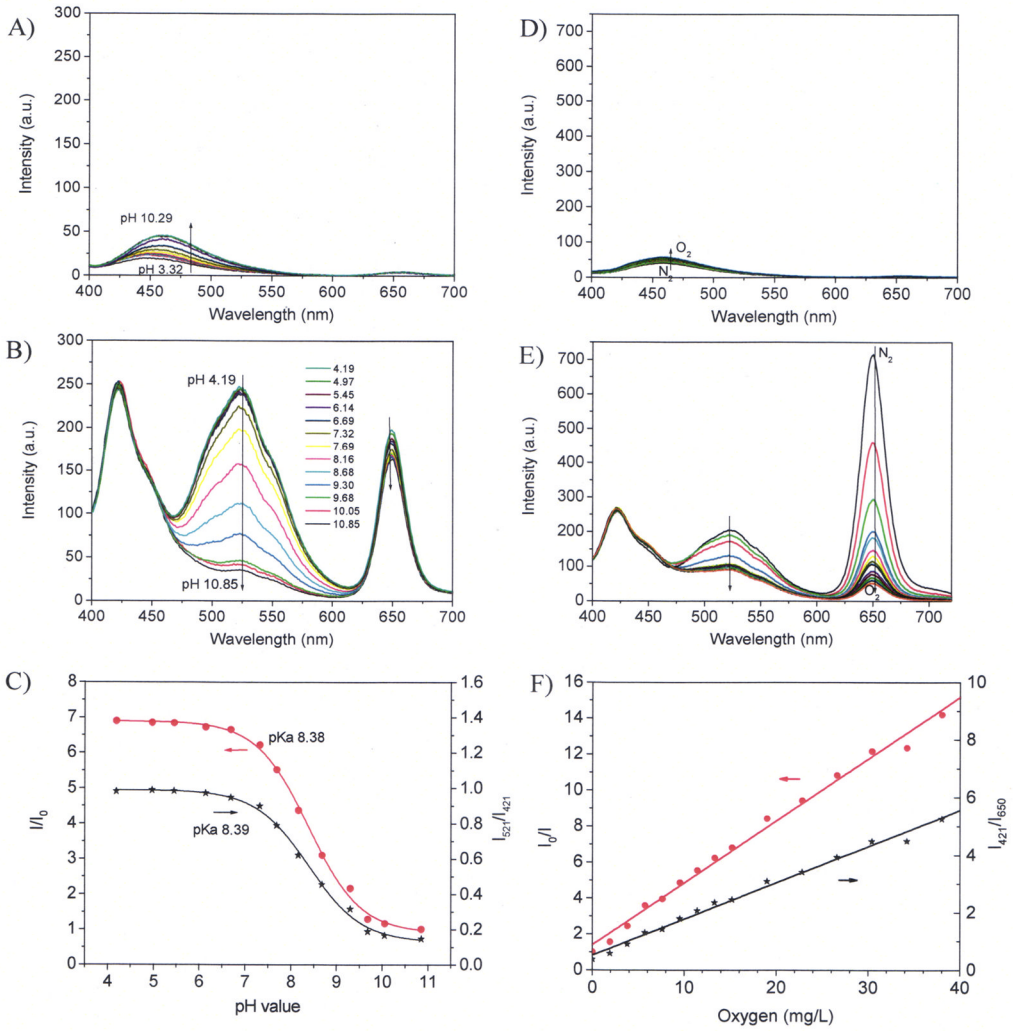

Figure 3.

Sensor responses with cyanobacteria (OD_{730} of 0.5). A) autofluorescence of cells at different pH values; B) pH responses of the sensor film with cells at different pH values; C) Sigmoidal plots of the pH responses with cells using the single pH sensor emission intensities at 521 nm and the ratiometric ratios at 521 nm and 421 nm; D) autofluorescence of cells via oxygen concentrations; E) emission spectral changes at different oxygen concentrations; F) Stern-Volmer plots of oxygen responses using the single oxygen sensor emission intensities at 650 nm and the ratiometric ratios at 650 nm and 421 nm.

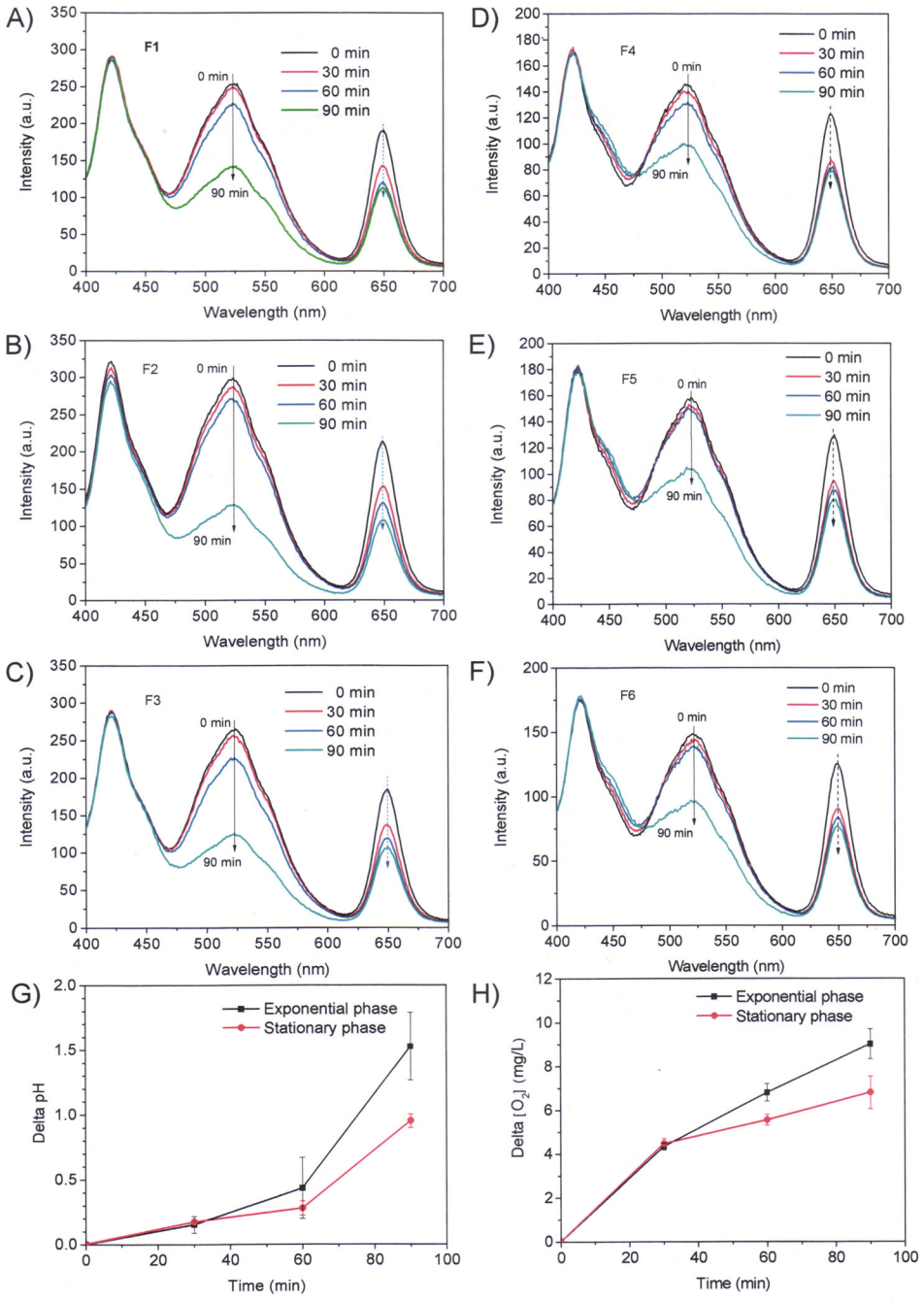

Figure 4.

Monitoring pH and oxygen changes using the optical sensors. A, B, and C are for the measurements at exponential phases at room temperature using three different films; D, E, and F are for the measurements at stationary phases at room temperature using three different films. G gives the time-dependent differences of pH values of the stationary phase and exponential phases. H gives the time-dependent differences of dissolved oxygen concentrations of the stationary phase and exponential phases. OD_{730} of the cell densities for these studies are 0.5.

Table 1

Comparison of pH and O_2 measurements using optical sensors and electrodes

		$t_{0\ min}$			$t_{90\ min}$		
		by sensors	**by electrodes**	**Difference** [a]	**by sensors**	**by electrodes**	**Difference** [a]
F1 [b]	pH	7.26	7.20	0.06	8.49	8.78	−0.29
	$[O_2]$ [d]	7.94	7.75	0.19	16.3	16.8	−0.5
F2 [b]	pH	6.91	7.20	−0.29	8.63	8.90	−0.27
	$[O_2]$ [d]	8.02	7.75	0.27	17.5	17.4	0.1
F3 [b]	pH	7.00	7.20	−0.20	8.63	8.81	−0.18
	$[O_2]$ [d]	8.35	7.75	0.6	16.7	16.1	0.6
F4 [c]	pH	7.38	7.29	0.09	8.35	8.39	−0.04
	$[O_2]$ [d]	6.95	7.06	−0.11	14.6	14.5	0.1
F5 [c]	pH	7.23	7.29	0.06	8.22	8.38	0.16
	$[O_2]$ [d]	6.84	7.06	−0.22	13.5	14.5	−1.0
F6 [c]	pH	7.36	7.29	0.07	8.25	8.42	−0.17
	$[O_2]$ [d]	6.99	7.06	−0.07	13.1	14.3	−1.2

[a] The difference was calculated by values measured by sensors – values measured by electrodes. Values calculated from the sensing films were based on the titration results of F1.

[b] F1, F2, and F3 are for exponential phases measurements.

[c] F4, F5, and F6 are for stationary phases measurements.

[d] $[O_2]$ was expressed in mg/L. Experiment was carried out at room temperature.